ARTICLE

Flexible and Metal-Free Light-Emitting Electrochemical Cells Based on Graphene and PEDOT-PSS as the Electrode Materials

Piotr Matyba,[†,⊥] Hisato Yamaguchi,[‡,⊥] Manish Chhowalla,[‡] Nathaniel D. Robinson,[§] and Ludvig Edman[†,*]

[†]The Organic Photonics and Electronics Group, Department of Physics, Umeå University, SE-901 87 Umeå, Sweden, [‡]Department of Materials Science and Engineering, Rutgers University, 607 Taylor Road, Piscataway, New Jersey 08854, United States, and [§]The Transport and Separations Group, Department of Physics, Chemistry and Biology, Linköping University, SE-58183 Linköping, Sweden. [⊥]These authors contributed equally to this work.

ABSTRACT We report flexible and metal-free light-emitting electrochemical cells (LECs) using exclusively solution-processed organic materials and illustrate interesting design opportunities offered by such conformable devices with transparent electrodes. Flexible LEC devices based on chemically derived graphene (CDG) as the cathode and poly(3,4-ethylenedioxythiophene) mixed with poly(styrenesulfonate) as the anode exhibit a low turn-on voltage for yellow light emission ($V = 2.8$ V) and a good efficiency 2.4 (4.0) cd/A at a brightness of 100 (50) cd/m^2. We also find that CDG is electrochemically inert over a wide potential range (+1.2 to −2.8 V *vs* ferrocene/ferrocenium) and exploit this property to demonstrate planar LEC devices with CDG as both the anode and the cathode.

KEYWORDS: light-emitting electrochemical cell · metal-free · flexible · solution processing · graphene · superyellow · PEDOT-PSS · doping · p−n junction

Organic electronics is a rapidly developing field that utilizes pristine and doped organic semiconductors (OSCs) to produce of a wide range of functional and novel devices.[1−9] One particularly tantalizing opportunity is the anticipated emergence of conformable, lightweight, and large-area emissive panels based solely on "green" and abundant OSC materials that are fabricated from solution using low-cost and scalable roll-to-roll processes. Such devices are often conceptualized as "light-emitting wallpaper".

The emissive technology *in vogue* within the organic electronics community is the organic light-emitting diode (OLED),[10−12] which has been introduced in a number of small-sized commercial applications.[13] OLEDs can be divided into SMOLEDs when the active material comprises small organic molecules and POLEDs when the active material is a conjugated polymer (CP). However, neither OLED technology is expected to fulfill the full wall-paper vision because SMOLEDs depend on expensive vacuum evaporation for the fabrication of (parts of) the active material, and POLEDs require the use of a low-work-function (and reactive) metal cathode that is incompatible with solution processing. Moreover, all OLEDs depend on very thin (∼100 nm) layers of active material with well-defined thicknesses, which are difficult to attain with low-cost solution fabrication.

In view of recent promising reports,[14−21] it appears plausible that an alternative, and significantly less studied, organic electronic device—the light-emitting electrochemical cell (LEC)—could fulfill the requirements necessary for light-emitting wallpaper-like applications to be realized. LECs utilize an ion- and electron-conducting blend as the active material sandwiched between the cathode and anode.[22−28] It has been demonstrated that a dynamic p−n junction doping structure can form *in situ* in the active material of LEC devices based on conjugated polymers.[29,30] The dynamic formation of doping brings the advantages that LECs, in contrast to OLEDs, can function efficiently independently of the work function of the electrodes and the thickness of the active material.[31−34] Moreover, Yu *et al.*[35] and Matyba *et al.*[36] have recently demonstrated that it is possible to fabricate LECs comprising solution-processable OSC compounds for both electrodes and the active material and that such metal-free devices can exhibit efficient light emission. Yu and co-workers[35] utilized a network of conducting carbon nanotubes for both the anode and the cathode, whereas Matyba and co-workers[36] used chemically derived graphene (CDG) for the cathode and a con-

*Address correspondence to ludvig.edman@physics.umu.se.

Received for review October 10, 2010 and accepted December 13, 2010.

Published online December 28, 2010. 10.1021/nn102704h

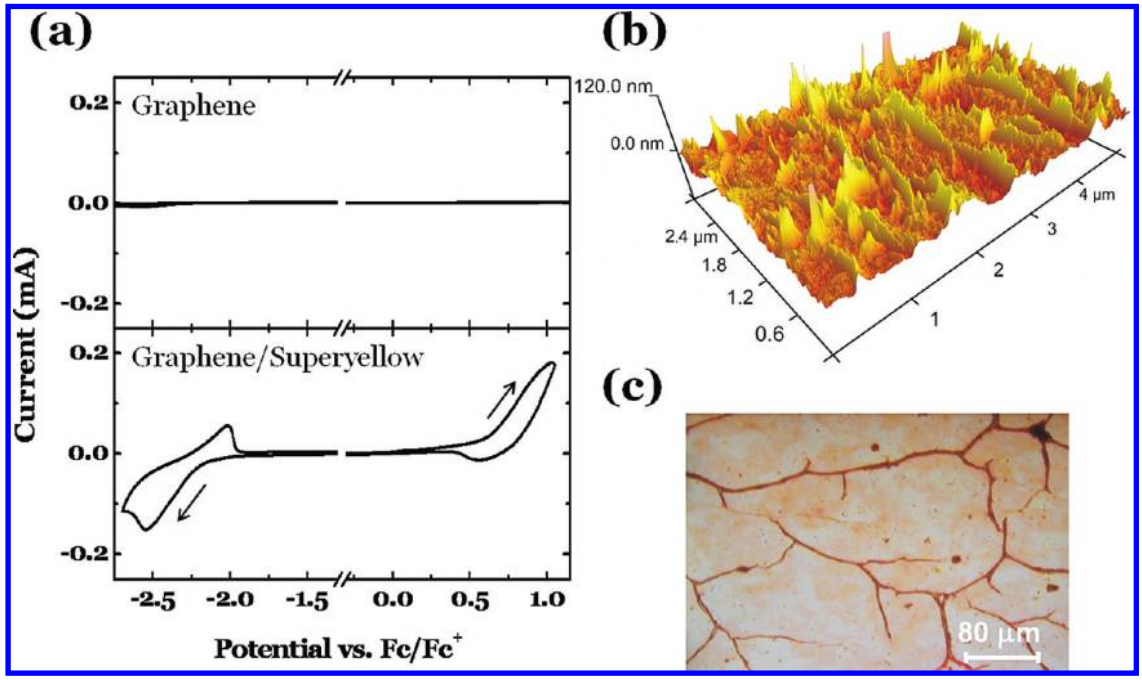

Figure 1. (a) Upper panel: CV recorded using a thin film of chemically derived graphene as the working electrode. Lower panel: CV recorded using a chemically derived graphene electrode coated with a thin film of the conjugated polymer superyellow as the working electrode. CV measurements were performed in 0.1 M $TBAPF_6$ in acetonitrile using a Pt disk as the counter electrode. The sweep rate was 50 mV/s. (b) An AFM topography image of a chemically derived graphene film on a quartz substrate. (c) A micrograph of the same chemically derived graphene film.

ducting polymer, poly(3,4-ethylenedioxythiophene) mixed with poly(styrenesulfonate) (PEDOT-PSS), for the anode.

In this article, we expand upon and develop the concept introduced by Matyba *et al*. We show that CDG exhibits a notably wide electrochemical stability window and utilize this for the realization of planar LEC devices with CDG as both the cathode and the anode and with interelectrode gaps of 2 mm. We further fabricate CDG on flexible polyethylene terephthalate (PET) substrates and, although the surface of such CDG films is found to be quite rough, we demonstrate flexible LEC sandwich cells that emit strong yellow light at low voltage and high efficiency (*e.g.*, 100 cd/m^2 at 4.5 V and 2.4 cd/A). Finally, as both electrodes in the flexible device are transparent, it is possible to design novel conformable emissive architectures. Here, we wrap a flexible LEC device around a thin capillary tube containing a dispersion of red-emitting quantum dots so that yellow light is emitted outward in the radial direction from the tube while red light is emitted along the tube's long axis.

During the initial operation of an LEC, ions within the active material redistribute in response to the applied voltage, *V*. If the voltage is equal to or larger than the band gap potential of the conjugated polymer, p-type doping is initiated at the anode and n-type doping is initiated at the cathode. With time, these two doped and highly conductive regions grow in size and eventually make contact under the formation of a light-emitting p−n junction structure in the bulk of the active material.[37,38] However, it is notable that this scenario represents the ideal operation of an LEC and that a plethora of undesired electrochemical side reactions also can take place. For instance, it has been demonstrated that the electrode material (as well as the electrolyte)[39] can take part in electrochemical side reactions during the operation of LEC devices at the expense of the desired doping reactions.[40] To alleviate, and ideally eliminate, these side reactions, it is advisible to employ electrode materials that are electrochemically inert in the voltage range spanned by the p-type (oxidation) and n-type (reduction) potentials of the CP. If this is not the case, then there is a significant risk that the electrode material will react electrochemically during LEC operation, resulting in the formation of side-reaction residues at the electrode interface(s) that can severely limit, or even halt, the operation of the device.

The upper panel in Figure 1a presents a cyclic voltammogram (CV) recorded on a CDG-coated quartz substrate over a wide potential interval that spans the p-type and n-type doping potentials of most conjugated polymers (+1.2 to −2.8 V *vs* ferrocene/ferrocenium, Fc/Fc^+). A careful inspection of the CV reveals a minor and reversible reduction event at −2.3 V *vs* Fc/Fc^+, with a peak current on the order of a few microamperes (*i.e.*, too small to be distinguishable in the panel). On the basis of the small magnitude and potential position of the reversible peak, we attribute it to reversible reduction of epoxy and/or hydroxyl groups that have been shown to remain within CDG following the synthesis process.[41−43] More importantly, however, we do not detect any significant or irreversible current peaks

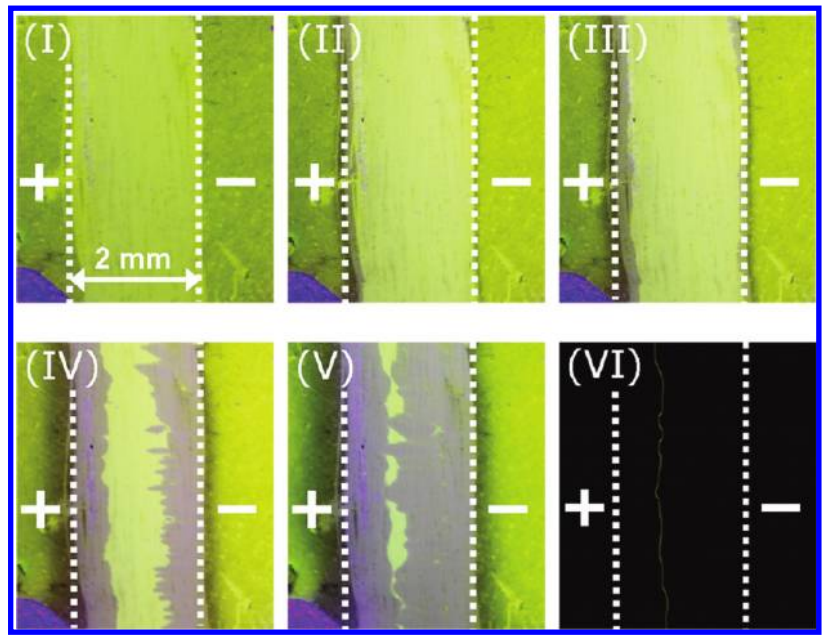

Figure 2. Sequence of photographs showing the initial operation of a planar LEC, comprising a {superyellow + PEO + KCF_3SO_3} active material positioned between two identical CDG electrodes. The interelectrode gap is 2 mm, and the device was driven at $V = 20$ V at a temperature of $T = 380$ K. The device was operated under UV illumination in a dark room so that the doping formation could be visualized as dark regions growing away from the electrode interfaces; the latter are identified by the vertical white dotted lines. The Roman numerals indicate the time at which the photographs were recorded: (I) $t = 0$ s, (II) $t = 2$ s, (III) $t = 4$ s, (IV) $t = 32$ s, (V) $t = 68$ s, and (VI) $t = 78$ s.

anywhere in the probed potential interval, which suggests that CDG could be appropriate for *both* the cathode and the anode in LEC applications.

This assumption is supported by the CV recorded on a CDG electrode coated with a film of the conjugated polymer superyellow, as presented in the lower panel in Figure 1a. The observed oxidation peak with an onset at +0.6 V *vs* Fc/Fc^+ can be attributed to p-type doping of superyellow, while the reduction peak with an onset at −2.2 V *vs* Fc/Fc^+ is attributed to n-type doping of superyellow, in agreement with a previous CV study on the same conjugated polymer using Au as the working electrode.[15] The fact that the return peaks exhibit a lower integrated magnitude than the forward peaks should not be taken as a sign of irreversibility of the doping reaction, as the doped (and, as a consequence, more hydrophilic) superyellow was observed to dissolve into the (hydrophilic) electrolyte during the CV measurements.

Figure 1b,c presents an AFM topography image and an optical micrograph, respectively, of a pristine CDG film on a quartz substrate. The AFM image discloses significant surface roughness with distinct elevated features up to 120 nm in height protruding from the surface of the CDG film (with an average thickness of 25 nm), whereas the optical micrograph reveals the existence of micrometer-sized branching wrinkles within the CDG film. The existence of such an uneven and inhomogeneous electrode surface corresponds to significant challenges for devices and applications that rely on uniform thin films for their operation. For instance, it is expected, and also recently demonstrated,[36] that OLED devices based on an uneven CDG film as the anode material suffer from electrical short circuits and/or uneven light emission. LECs are, in contrast, remarkably tolerant toward structural features at the surface of the electrode, as the *in situ* formation of doped regions results in a light-emitting p−n junction physically isolated from the uneven surface within a thick layer of active material (active material thickness > electrode surface roughness). We will return to this topic later but will first consider the opportunities that the wide electrochemical stability window of CDG offers for the electrode selection in LEC devices.

The definite proof for that the wide electrochemical stability window of CDG indeed allows it to function as both the anode and the cathode in LEC applications is provided by experiments on open planar devices, as shown in Figure 2. The devices were fabricated by making a scratch in a CDG film deposited on a quartz substrate using a razor blade, letting the scratch define the interelectrode gap; here, $d \sim 2$ mm. (Alternatively, one could likely establish the interelectrode gap in the graphene film *via* the heating action of an intense laser beam or lift-off photolithography.) A thin film comprising a blend of superyellow and a {PEO + KCF_3SO_3} electrolyte was deposited (from solution) on top of the electrodes and the gap between them to complete the device assembly.

The photographs presented in Figure 2 were recorded during the operation of such a planar LEC with a CDG anode (left) and a CDG cathode (right). The de-

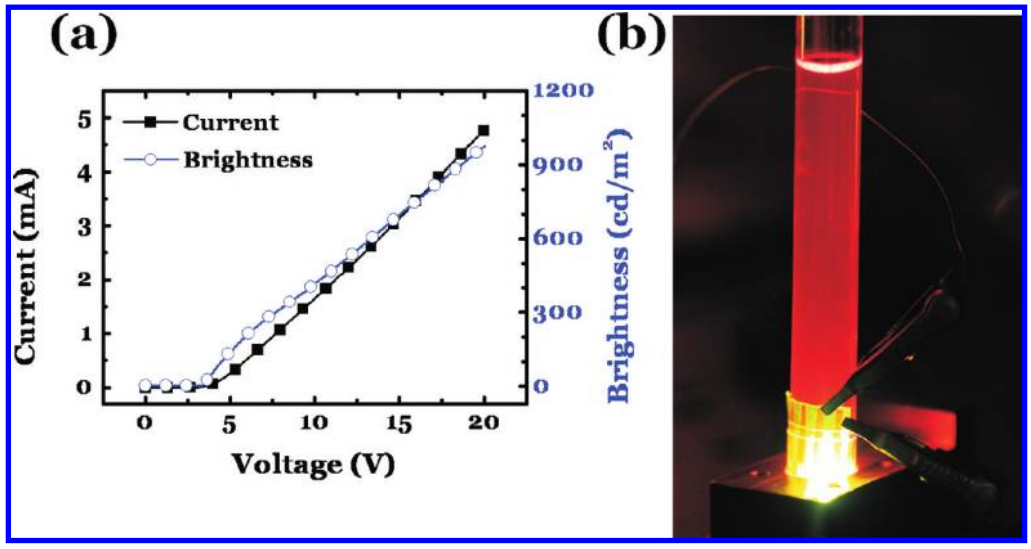

Figure 3. Flexible PEDOT-PSS/{superyellow + PEO + KCF_3SO_3}/CDG LEC on a PET substrate. Note that both electrodes are transparent and that the device contains no metal. (a) Current−brightness−voltage graph for the flexible device, with the brightness recorded through the transparent CDG cathode. The voltage sweep rate was 0.1 V/s. (b) Photograph of a yellow-emitting flexible LEC, wrapped around a vial containing a dispersion of red-emitting quantum dots. The photograph was taken in a dark room, and the red emission from the vial stems from excitation of the quantum dots by the yellow emission from the LEC through the transparent CDG cathode.

vice was driven at $V = 20$ V at $T = 380$ K and imaged under UV illumination in a dark room. The latter allows doping to be visualized as dark regions because the UV-excited photoluminescence of superyellow[15,44] (and other conjugated polymers) is efficiently quenched by doping.[33,34,45,46] Photograph (I) shows the device when the voltage was first applied and the active material is undoped (and accordingly, fully photoluminescent). The consecutive photographs (II) and (III) depict the onset of p-type doping (from the anode) and n-type doping (from the cathode), respectively. The delay in the appearance of n-type doping with respect to p-type doping is ~2−3 s and can be attributed to an initial electrochemical side reaction involving the {PEO + KCF_3SO_3} electrolyte at the negative cathode.[39] Photograph (IV) shows the doping after it has traversed approximately half of the interelectrode gap, and photograph (V) depicts the fronts when they barely have made contact and the p−n junction is about to form (or has already formed in a few short regions). Photograph (VI) finally shows the light emission from a fully formed p−n junction (without UV illumination). The light emission was invariably weak and could only be detected by setting the probing camera to high sensitivity. We note that this is consistent with previous results on planar LECs based on superyellow and using Au as the electrode material,[15,47] but we also point out that more conventional sandwich-cell LECs based on superyellow can be very bright and efficient[15−17,20,48] (see also Figure 3 and the accompanying text below).

As mentioned previously, we also fabricated CDG on plastic PET substrates to obtain *flexible and metal-free* LEC devices. Typically, chemical reduction yielding the lowest sheet resistance is achieved for CDG thin films annealed at 1000 °C. The key challenge in this work was to transfer the fully reduced films onto plastic substrates. The detailed CDG and device fabrication procedures are outlined in the Methods section. Figure 3a presents data recorded on a PEDOT-PSS/{superyellow + PEO + KCF_3SO_3}/CDG sandwich cell mounted on a flexible PET substrate during a voltage sweep experiment ($dV/dt = 0.1$ V/s) at room temperature. The device turns on and emits light (with a brightness > 1 cd/m^2) at a relatively low voltage of $V = 2.8$ V and reaches a maximum brightness of 1000 cd/m^2 at $V = 20$ V. The brightness in Figure 3a was measured from the CDG-cathode/PET-substrate side, but both electrodes in this device are transparent. Thus, it is appropriate to account for both the "top" emission through the PEDOT-PSS anode and the "bottom" emission through the CDG-cathode/PET-substrate when calculating the device efficiency. For this device, we found the maximum current efficacy to be 4.0 (2.4) cd/A and the maximum power efficacy to be 2.8 (2.4) lm/W at a brightness of 50 (100) cd/m^2. The emission from the device appears uniform to the observer, which is highly noteworthy given the uneven surface of the CDG film (see Figure 1b,c) and important for many applications. We have also repeatedly bent such a flexible device to a radius of ~5 mm, and we find that the emission remains homogeneous and constant over the entire light-emitting area during and following the bending.

The omnidirectional emission and the flexible nature of this LEC architecture enable interesting design opportunities. Figure 3b presents a photograph of a flexible LEC device wrapped around a glass tube with a diameter of 6 mm. The glass tube was filled with a

water suspension of CdSe/ZnS quantum dots (QDs), which was selected based on two criteria: (i) the QD absorption should exhibit a good spectral overlap with the yellow emission from the LEC and (ii) the QDs should exhibit strong luminescence. With an appropriately designed system, it was anticipated that the inward light emission from the bent LEC device, through the CDG-cathode/PET-substrate side, would optically excite the QDs so that they, in turn, could emit red light. This is indeed observed in the photograph in Figure 3b, which was recorded in a dark room. The yellow emission originates from the light escaping the LEC device through the PEDOT-PSS anode, whereas the red emission stems from the optically excited QDs dispersed within the glass tube.

To summarize, graphene is demonstrated to be a highly appropriate and versatile material for metal-free LEC applications, as its wide electrochemical stability window, optical transparency, and high conductivity make it suitable as both the anode and the cathode. Moreover, the unique operational mechanism of LECs, which involves *in situ* doping and p−n junction formation, effectively alleviates problems that could stem from challenges involving the solution processing of graphene, for example, in this case, a rather rough surface. We finally exemplify the potential of our herein demonstrated metal-free and flexible LECs in novel and functional architectures by introducing a device architecture, which emits significant and efficient light of two colors at low voltage.

METHODS

Graphite powders (Branwell Graphite Ltd.) with a particle size > 425 μm were exfoliated *via* a modified Hummer's method.[49] The acid and other reactants were removed from the oxidized graphite powders by repeated washing in deionized water, whereas unexfoliated graphite particles were removed by mild centrifugation. The graphene oxide (GO) aqueous suspension was then diluted and vacuum filtered onto cellulose paper filters.[50] The GO films were initially deposited onto quartz substrates for thermal reduction at 1000 °C for 15 min in an Ar/H_2 environment (Ar, 90%; H_2, 10%). The films were preannealed at 200 °C in vacuum overnight to minimize the possible loss of carbon atoms upon annealing. The resulting chemically derived graphene (CDG) electrodes had a sheet resistance of approximately 5 kΩ/sq.

For the attainment of flexible electrodes, the CDG films were transferred to flexible polyethylene terephthalate (PET) substrates *via* lift-off.[51,52] The transfer was achieved by spin-coating poly(methyl methacrylate) (PMMA) on top of the CDG film, where after the assembly was heated at 120−170 °C for 1−3 h. After the heating step, the PMMA/CDG/quartz assembly was submerged in sodium hydroxide (NaOH) for the delamination of the PMMA/CDG from the quartz. The speed of the lift-off was controlled by modifying the NaOH concentration. The delaminated PMMA/CDG membrane was transferred to the flexible PET substrate, followed by rinsing in acetone for removal of the PMMA, leaving a uniform CDG thin film for use. The effect of the transfer process on the sheet resistance of CDG films was minimal.

The conjugated polymer is commercially available and known as "superyellow" (Merck catalogue no. PDY-132). Superyellow, polyethylene oxide ($M_w = 5 \times 10^6$ g/mol, Aldrich), and KCF_3SO_3 (Alfa Aesar, purity = 98%) were separately dissolved in cyclohexanone (Aldrich, purity = 99.8%) in a concentration of 5 mg/mL. For LEC device fabrication, the three master solutions were mixed together in a volume ratio of superyellow/PEO/KCF_3SO_3 = 1.0:1.35:0.25 to form an active-material solution.

For the CV measurements, the electrolyte solution was prepared by dissolving tetrabutylammonium hexafluorophosphate ($TBAPF_6$, >99%, Fluka) in anhydrous acetonitrile (>99.8%, Aldrich) in a concentration of 0.1 M. A silver wire served as the quasi-reference electrode, and a platinum disk was used as the counter electrode. Directly after each (cathodic or anodic) CV scan, a calibration scan was run with a small amount of bis-(g-cyclopentadienyl)iron(II) (ferrocene, >98%, Fluka) added to the electrolyte, yielding a $\sim 10^{-4}$ M ferrocene concentration in CH_3CN. All potentials in the CV measurements are reported *versus* the ferrocene/ferrocenium ion (Fc/Fc^+) reference redox system. The onset potentials for oxidation and reduction were calculated as the intersection of the baseline with the tangent of the current at the half-maximum of the peak. The superyellow-coated working electrode was prepared by spin-coating the superyellow solution onto the CDG-coated quartz substrate at 800 rpm for 60 s and at 2000 rpm for 10 s. All CV measurements were performed in a glovebox ($[O_2]$, $[H_2O] < 1$ ppm).

The atomic force microscopy (AFM) images of CDG films on quartz substrates were recorded in tapping mode using a MultiMode SPM microscope with a Nanoscope IV Controller (Veeco Metrology) operating under ambient conditions. Etched silicon tips, with a nominal radius of ∼10 nm and mounted on a 180 μm long Al-coated cantilever, were used for the measurements (OTESPA, $f_0 = 320-370$ Hz, $k = 12-103$ N/m, Veeco Probes). The probes were driven below their resonance frequency (by ∼10%) in the 300−330 Hz range. The 3D topography images were recorded using the NanoScope software and a custom written Matlab script.

Planar LEC devices were fabricated by establishing a 2 mm interelectrode gap in a CDG film on a quartz substrate using a razor blade. The active material solution was spin-coated on top of the gap at 800 rpm for 60 s and 2000 rpm for 10 s so that an active material film with a thickness of 120 nm was attained. The devices were, thereafter, dried on a hot plate for $T = 360$ K for 12 h. The latter two steps were executed under a N_2 atmosphere in a glovebox. The devices were then transferred to an optical-access vacuum chamber for characterization. Immediately prior to a measurement, the device was further dried under a vacuum of $\sim 5 \times 10^{-6}$ mBar at $T = 380$ K for at least 2 h. A computer-controlled source meter (Keithley 2400) was applying a constant voltage of $V = 20$ V and measuring the resulting current. The testing was performed at $T = 380$ K and under UV illumination (peak wavelength = 360 nm). Photographs were recorded with an SLR camera (Canon EOS 20) equipped with a macrolens (60 mm, f/2.8) and a teleconverter (2×).

Flexible sandwich cells were fabricated by drop-casting the active material solution onto 1×1 cm^2 CDG-coated PET substrates. The resulting active material film with a thickness of 1−2 μm was dried on a hot plate at $T = 360$ K for 12 h. A shadow mask was created by establishing a mesh pattern, comprising four 5×1 mm^2 openings, in a thin cellophane film. The shadow mask was placed on top of the active material and attached to the edges of the substrate. The entire shadow mask−substrate assembly was heated at $T = 360$ K for ≥10 min, where after a viscous PEDOT-PSS dispersion (Clevios S V3, H. C. Starck) was coated on top of the mask using the edge of a glass microscope slide that rested on the mask. The mask was, thereafter, removed, and the device dried on a hot plate at $T = 390$ K for ≥12 h. The thickness of the dry PEDOT-PSS top electrode was ∼5−10 μm. A drop of a conductive silver paste was added to the edge of the PEDOT-PSS top and CDG bottom electrodes to establish good electrical contact pads. The entire device was placed in a sample holder that contacted the pads and allowed each 5×1 mm^2 "pixel" to be addressed and measured individually. The devices were driven by, and current measured with, a Keithley 2400 source meter. The brightness was measured using a calibrated

photodiode with an eye response filter (Hamamatsu Photonics) connected through a current-to-voltage amplifier to an HP 34401A meter. The photograph in Figure 3b was recorded on such a flexible LEC device wrapped around a glass tube with a diameter of 7 mm. The glass tube was filled with a suspension of quantum dots (Lumidot CdSe/ZnS, emission peak = 610 nm), and the photograph was taken in darkness. All LEC fabrications and measurements were performed in N_2-filled gloveboxes ([O_2], [H_2O] $<$ 1 ppm).

Acknowledgment. L.E. and P.M. are grateful to Kempestiftelserna, Carl Tryggers Stiftelse, and the Swedish Research Council (Vetenskapsrådet) for financial support. L.E. is a "Royal Swedish Academy of Sciences Research Fellow" supported by a grant from the Knut and Alice Wallenberg Foundation. N.D.R. recognizes financial support from the Swedish Research Council (Vetenskapsrådet). H.Y. and M.C. acknowledge National Science Foundation CAREER Award (ECS 0543867). M.C. acknowledges support from the Royal Society through the Wolfson Merit Award.

REFERENCES AND NOTES

1. Forrest, S. R. The Path To Ubiquitous and Low-Cost Organic Electronic Appliances On Plastic. *Nature* **2004**, *428*, 911–918.
2. Malliaras, G.; Friend, R. An Organic Electronics Primer. *Phys. Today* **2005**, *58*, 53–58.
3. Leger, J. M. Organic Electronics: The Ions Have It. *Adv. Mater.* **2008**, *20*, 837–841.
4. Holt, A. L.; Wehner, J. G. A.; Hammp, A.; Morse, D. E. Plastic Transmissive Infrared Electrochromic Devices. *Macromol. Chem. Phys.* **2010**, *211*, 1701–1707.
5. Yumusak, C.; Sariciftci, N. S. Organic Electrochemical Light Emitting Field Effect Transistors. *Appl. Phys. Lett.* **2010**, *97*, 033302.
6. Lin, F. D.; Walker, E. M.; Lonergan, M. C. Photochemical Doping of an Adaptive Mix-Conducting p-n Junction. *J. Phys. Chem. Lett.* **2010**, *1*, 720–723.
7. Zhao, J. H.; Thomson, D. J.; Pilapil, M.; Pillai, R. G.; Rahman, G. M. A.; Freund, M. S. Field Enhanced Charge Carrier Reconfiguration in Electronic and Ionic Coupled Dynamic Polymer Resistive Memory. *Nanotechnology* **2010**, *21*, 134003–134010.
8. Zakhidov, A. A.; Jung, B.; Slinker, J. D.; Abruna, H. D.; Malliaras, G. G. A Light-Emitting Memristor. *Org. Electron.* **2010**, *11*, 150–153.
9. Dzwilewski, A.; Matyba, P.; Edman, L. Facile Fabrication of Efficient Organic CMOS Circuits. *J. Phys. Chem. B* **2010**, *114*, 135–140.
10. Kohnen, A.; Irion, M.; Gather, M. C.; Rehmann, N.; Zacharias, P.; Meerholz, K. Highly Color-Stable Solution-Processed Multilayer WOLEDs for Lighting Application. *J. Mater. Chem.* **2010**, *20*, 3301–3306.
11. Harding, M. J.; Poplavskyy, D.; Choong, V. E.; So, F.; Campbell, A. J. Variations in Hole Injection due to Fast and Slow Interfacial Traps in Polymer Light-Emitting Diodes with Interlayers. *Adv. Funct. Mater.* **2010**, *20*, 119–130.
12. Wallikewitz, B. H.; Hertel, D.; Meerholz, K. Cross-Linkable Polyspirobifluorenes: A Material Class Featuring Good OLED Performance and Low Amplified Spontaneous Emission Thresholds. *Chem. Mater.* **2009**, *21*, 2912–2919.
13. He, G. F.; Rothe, C.; Murano, S.; Werner, A.; Zeika, O.; Birnstock, J. White Stacked OLED with 38 lm/W and 100,000-h Lifetime at 1000 cd/m(2) for Display and Lighting Applications. *J. Soc. Inf. Disp.* **2009**, *17*, 159–165.
14. Fang, J. F.; Matyba, P.; Edman, L. The Design and Realization of Flexible, Long-Lived Light-Emitting Electrochemical Cells. *Adv. Funct. Mater.* **2009**, *19*, 2671–2676.
15. Sandstrom, A.; Matyba, P.; Edman, L. Yellow-Green Light-Emitting Electrochemical Cells with Long Lifetime and High Efficiency. *Appl. Phys. Lett.* **2010**, *96*, 053303.
16. Shao, Y.; Bazan, G. C.; Heeger, A. J. Long-Lifetime Polymer Light-Emitting Electrochemical Cells. *Adv. Mater.* **2007**, *19*, 365.
17. Shao, Y.; Gong, X.; Heeger, A. J.; Liu, M.; Jen, A. K. Y. Long-Lifetime Polymer Light-Emitting Electrochemical Cells Fabricated with Crosslinked Hole-Transport Layers. *Adv. Mater.* **2009**, *21*, 1972–1975.
18. Mauthner, G.; Landfester, K.; Kock, A.; Bruckl, H.; Kast, M.; Stepper, C.; List, E. J. W. Inkjet Printed Surface Cell Light-Emitting Devices from a Water-Based Polymer Dispersion. *Org. Electron.* **2008**, *9*, 164–170.
19. Hoven, C. V.; Wang, H. P.; Elbing, M.; Garner, L.; Winkelhaus, D.; Bazan, G. C. Chemically Fixed p−n Heterojunctions for Polymer Electronics by Means of Covalent B−F Bond Formation. *Nat. Mater.* **2010**, *9*, 249–252.
20. Tang, S.; Edman, L. Quest for an Appropriate Electrolyte for High-Performance Light-Emitting Electrochemical Cells. *J. Phys. Chem. Lett.* **2010**, *1*, 2727–2732.
21. Costa, R. D.; Orti, E.; Bolink, H. J.; Graber, S.; Housecroft, C. E.; Constable, E. C. Efficient and Long-Living Light-Emitting Electrochemical Cells. *Adv. Funct. Mater.* **2010**, *20*, 1511–1520.
22. Latini, G.; Winroth, G.; Brovelli, S.; McDonnell, S. O.; Anderson, H. L.; Mativetsky, J. M.; Samori, P.; Cacialli, F. Enhanced Luminescence Properties Of Highly Threaded Conjugated Polyelectrolytes with Potassium Counter-Ions Upon Blending with Poly(ethylene oxide). *J. Appl. Phys.* **2010**, *107*, 124509.
23. Inganas, O. Hybrid Electronics and Electrochemistry with Conjugated Polymers. *Chem. Soc. Rev.* **2010**, *39*, 2633–2642.
24. Marcilla, R.; Mecerreyes, D.; Winroth, G.; Brovelli, S.; Yebra, M. D. R.; Cacialli, F. Light-Emitting Electrochemical Cells Using Polymeric Ionic Liquid/Polyfluorene Blends as Luminescent Material. *Appl. Phys. Lett.* **2010**, *96*, 043308.
25. Hu, L.; Xu, G. Applications and Trends in Electrochemiluminescence. *Chem. Soc. Rev.* **2010**, *39*, 3275–3304.
26. He, L.; Duan, L. A.; Qiao, J. A.; Dong, G. F.; Wang, L. D.; Qiu, Y. Highly Efficient Blue-Green and White Light-Emitting Electrochemical Cells Based on a Cationic Iridium Complex with a Bulky Side Group. *Chem. Mater.* **2010**, *22*, 3535–3542.
27. Heo, H. J.; Nagamura, T. Synthesis and Physical Properties of Polyfluorene Derivative with Imidazolium Units. *Mol. Cryst. Liq. Cryst.* **2010**, *520*, 277–285.
28. Costa, R. D.; Orti, E.; Bolink, H. J.; Graber, S.; Housecroft, C. E.; Constable, E. C. Intramolecular π-Stacking in a Phenylpyrazole-Based Iridium Complex and Its Use in Light-Emitting Electrochemical Cells. *J. Am. Chem. Soc.* **2010**, *132*, 5978.
29. Matyba, P.; Maturova, K.; Kemerink, M.; Robinson, N. D.; Edman, L. The Dynamic Organic p−n Junction. *Nat. Mater.* **2009**, *8*, 672–676.
30. Rodovsky, D. B.; Reid, O. G.; Pingree, L. S. C.; Ginger, D. S. Concerted Emission and Local Potentiometry of Light-Emitting Electrochemical Cells. *ACS Nano* **2010**, *4*, 2673–2680.
31. Pei, Q. B.; Yang, Y.; Yu, G.; Zhang, C.; Heeger, A. J. Polymer Light-Emitting Electrochemical Cells: In Situ Formation of a Light-Emitting p−n Junction. *J. Am. Chem. Soc.* **1996**, *118*, 3922–3929.
32. Pei, Q. B.; Yu, G.; Zhang, C.; Yang, Y.; Heeger, A. J. Polymer Light-Emitting Electrochemical-Cells. *Science* **1995**, *269*, 1086–1088.
33. Shin, J. H.; Edman, L. Light-Emitting Electrochemical Cells with Millimeter-Sized Interelectrode Gap: Low-Voltage Operation at Room Temperature. *J. Am. Chem. Soc.* **2006**, *128*, 15568–15569.
34. Gao, J.; Dane, J. Planar Polymer Light-Emitting Electrochemical Cells With Extremely Large Interelectrode Spacing. *Appl. Phys. Lett.* **2003**, *83*, 3027–3029.
35. Yu, Z. B.; Hu, L. B.; Liu, Z. T.; Sun, M. L.; Wang, M. L.; Gruner, G.; Pei, Q. B. Fully Bendable Polymer Light Emitting Devices With Carbon Nanotubes as Cathode and Anode. *Appl. Phys. Lett.* **2009**, *95*, 203304.

36. Matyba, P.; Yamaguchi, H.; Eda, G.; Chhowalla, M.; Edman, L.; Robinson, N. D. Graphene and Mobile Ions: The Key to All-Plastic, Solution-Processed Light-Emitting Devices. *ACS Nano* **2010**, *4*, 637–642.
37. Sun, Q. J.; Li, Y. F.; Pei, Q. B. Polymer Light-Emitting Electrochemical Cells for High-Efficiency Low-Voltage Electroluminescent Devices. *J. Disp. Technol.* **2007**, *3*, 211–224.
38. Edman, L. Bringing Light To Solid-State Electrolytes: The Polymer Light-Emitting Electrochemical Cell. *Electrochim. Acta* **2005**, *50*, 3878–3885.
39. Fang, J.; Matyba, P.; Robinson, N. D.; Edman, L. Identifying and Alleviating Electrochemical Side-Reactions In Light-Emitting Electrochemical Cells. *J. Am. Chem. Soc.* **2008**, *130*, 4562–4568.
40. Shin, J. H.; Matyba, P.; Robinson, N. D.; Edman, L. The Influence of Electrodes on The Performance of Light-Emitting Electrochemical Cells. *Electrochim. Acta* **2007**, *52*, 6456–6462.
41. Stankovich, S.; Dikin, D. A.; Piner, R. D.; Kohlhaas, K. A.; Kleinhammes, A.; Jia, Y.; Wu, Y.; Nguyen, S. T.; Ruoff, R. S. Synthesis of Graphene-Based Nanosheets via Chemical Reduction of Exfoliated Graphite Oxide. *Carbon* **2007**, *45*, 1558.
42. Boujlel, K.; Simonet, J. Cathodic Cleavage of Carbon-Oxygen Bonds. Direct and Indirect Electrochemical Reduction of Epoxides. *Electrochim. Acta* **1979**, *24*, 481–487.
43. Bagri, A.; Mattevi, C.; Acik, M.; Chabal, Y. J.; Chhowalla, M.; Shenoy, V. B. Structural Evolution During The Reduction of Chemically Derived Graphene Oxide. *Nat. Chem.* **2010**, *2*, 581–587.
44. Snedden, E. W.; Cury, L. A.; Bourdakos, K. N.; Monkman, A. P. High Photoluminescence Quantum Yield Due To Intramolecular Energy Transfer In The Super Yellow Conjugated Copolymer. *Chem. Phys. Lett.* **2010**, *490*, 76–79.
45. Hu, Y. F.; Gao, J. Direct Probing of a Polymer Electrolyte/Luminescent Conjugated Polymer Mixed Ionic/Electronic Conductor. *J. Am. Chem. Soc.* **2009**, *131*, 18236.
46. Gao, J.; Dane, J. Imaging The Doping and Electroluminescence In Extremely Large Planar Polymer Light-Emitting Electrochemical Cells. *J. Appl. Phys.* **2005**, *98*, 063513.
47. Sandstrom, A.; Matyba, P.; Inganas, O.; Edman, L. Separating Ion and Electron Transport: The Bilayer Light-Emitting Electrochemical Cell. *J. Am. Chem. Soc.* **2010**, *132*, 6646.
48. Shao, Y.; Bazan, G. C.; Heeger, A. J. LED to LEC Transition Behavior in Polymer Light-Emitting Devices. *Adv. Mater.* **2008**, *20*, 1191–1193.
49. Hirata, M.; Gotou, T.; Horiuchi, S.; Fujiwara, M.; Ohba, M. Thin-Film Particles of Graphite Oxide 1: High-Yield Synthesis And Flexibility of the Particles. *Carbon* **2004**, *42*, 2929–2937.
50. Eda, G.; Fanchini, G.; Chhowalla, M. Large-Area Ultrathin Films of Reduced Graphene Oxide as a Transparent and Flexible Electronic Material. *Nat. Nanotechnol.* **2008**, *3*, 270–274.
51. Eda, G.; Chhowalla, M. Chemically Derived Graphene Oxide: Towards Large-Area Thin-Film Electronics and Optoelectronics. *Adv. Mater.* **2010**, *22*, 2392–2415.
52. Yamaguchi, H.; Eda, G.; Mattevi, C.; Kim, H.; Chhowalla, M. Highly Uniform 300 mm Wafer-Scale Deposition of Single and Multilayered Chemically Derived Graphene Thin Films. *ACS Nano* **2010**, *4*, 524–528.